

## THE NATURAL CONVECTIVE GRAPHENE OXIDE NANOFLUID-FLOW IN AN UPRIGHT SQUEEZING CHANNEL

by

**Malik Z. ULLAH<sup>a</sup>, Taza GUL<sup>b</sup>, Ali S. ALSHOMRANI<sup>a</sup>,  
and Dumitru BALEANU<sup>c,d\*</sup>**

<sup>a</sup>Department of Mathematics, King Abdul Aziz University, Jeddah, Saudi Arabia

<sup>b</sup>Department of Mathematics, City University of Science and Information Technology,  
Peshawar, Pakistan

<sup>c</sup>Department of Mathematics, Faculty of Arts and Sciences, Cankaya University,  
Ankara, Turkey

<sup>d</sup>Institute of Space Sciences, Magurele-Bucharest, Romania

Original scientific paper

<https://doi.org/10.2298/TSCI190623362U>

*The 3-D flow of water based graphene oxide (GO-W) and ethylene glycol based graphene oxide (GO-EG) nanofluids amongst the binary upright and parallel plates is considered. The unsteady movement of the nanofluid is associated with the porous medium and the unbroken magnetic field is executed in the perpendicular track of the flow field. The basic governing equations have been altered using the Von Karman transformation, including the natural-convection in the downward direction. The solution for the modeled problem has been attained by means of optimal homotopy analysis method (OHAM). The influence of the physical parameters on the momentum boundary-layer, pressure and temperature fields is mainly focused. Moreover, the comparison of the GO-W and GO-EG nanofluids under the impact of physical constraints have been analyzed graphically and numerically. The imperative physical constraints of the drag force and heat transfer rate have been computed and conferred. The consequences have been validated using the error analysis and the obtained outcomes have been shown and discussed.*

Key words: ethylene glycol, GO-W porous medium, OHAM technique, natural convection, two vertical and parallel plates, MHD, water

### Introduction

The Chinese scientist Choi [1] is the pioneer to adopt the idea of nanoparticles and its thermophysical performance. The technological importance and the utilization of nanoparticles in nanotechnology were conferred by Choi *et al.* [2]. The thermophoretic and Brownian motion effects of the nanofluid have been examined by Buongiorno [3]. The shape of the nanosized particles rather than the spherical with new physical properties has been studied by Timofeeva *et al.* [4]. The efforts done by the researchers to define a comparative model for the improvement of the thermal conductivities. Maxwell [5], Jeffery [6], Davis [7], Lu and Lin [8], and Hamilton and Crosser [9] are the well-known thermal conductivity models and used in most of the mathematical models related to the problems occurring in the field of engineering and technologies. Sheikholeslami and Ganji [10] analyzed nanofluid-flow among parallel plates under the assumption of Brownian motion properties. Sheikholeslami and Ganji [11, 12] discussed

\* Corresponding author, e-mail: [dumitru@cankaya.edu.tr](mailto:dumitru@cankaya.edu.tr)

the nanofluid-flow in a square enclosure and copper nanoparticles with water amid in parallel channels. Sheikholeslami *et al.* [13] examined the fluid-flow in parallel plates and rotating system under the effect of MHD and heat source. Mahmoodi and Kandelousi [14] studied the analysis of hypothermal behavior and entropy generation under the effect of thermal radiation. Ellahi *et al.* [15] have used the new idea to study the shape of nanoparticles in a porous medium. They mentioned the entropy analysis of the different shapes of nanosized spherical particles. To discuss cylindrical shaped particles Akber and Butt [16] presented a unique type of flow of Cu-water nanofluids using platelet-, brick and cylindrical particles. The nature of different sized nanoparticles under the influence of porous media and mixed convection is scrutinized by Ellahi *et al.* [17]. Sheikholeslami *et al.* [18] very nicely discussed and presented a fresh idea to the fluid-flows among parallel plates. Mahmoodi and Kandelousi [19] discussed a comprehensive analysis of aluminum nanoparticles and kerosene oil under the influence of heat sources in parallel rotating plates. The similarity transformations are used to simplify the basic flow equations without disturbing the physical nature of the problems. Karman [20] have used the similarity transformation for the 2- and 3-D flow problems. To discuss more comprehensively, Sheikholeslami and Ganji [21] provide a detailed information, and take 3-D rotating plates. Rashidi *et al.* [22] described the effect of MHD in the fluid-flow model. They discussed briefly the influence of  $\gamma\text{Al}_2\text{O}_3\text{-C}_2\text{H}_6$  nanofluids the numerical value of physical parameters and graphical discussion section also included in their study. Ahmed *et al.* [23] fruitfully discussed  $\gamma\text{Al}_2\text{O}_3\text{-H}_2\text{O}$  and  $\gamma\text{Al}_2\text{O}_3\text{-C}_2\text{H}_6$  nanofluid squeezed flow among parallel plates. In valuation of the upstairs important conversation the aim of this work is to study the nanofluid-flow of the water and ethylene glycol-based graphene oxide (GO-W/GO-EG) nanofluid among the two parallel plates for the heat transfer enrichment applications. The medium between the plates is considered porous and the flow nature is unsteady under the influence of magnetic field. The results of the proposed problem have been obtained using the OHAM.

Consider the incompressible unsteady water and ethylene glycol-based graphene oxide MHD nanofluids flow amongst the two upright plates. The medium among the plates is considered porous and the plates are settled at  $y = 0$  and at  $D = \{[v_f(1 - \alpha t)]/a\}^{1/2}$ . The plate at  $y = 0$  is extended in the  $x$  direction with unsteady velocity  $U_0 = ax/(1 - \alpha t)$  and the plate at  $D$  is squeezing the nanofluid with velocity  $V_h = dD/dt$  along the negative  $y$  axis. The plates are placed vertically in the  $xz$  plane in a Cartesian co-ordinate system and the fluid-flow is along the  $z$ -axis. The  $y$ -axis is perpendicular to the plates. The nanofluid-flow is in the downward  $z$ -direction due the existence of gravity force. The velocity components  $u, v, w$  are acting along the  $x, y, z$ -directions. Assume that  $T_0$  and  $T_D$  are the temperatures of the plates at  $y = 0$  and  $y = D$ . Here  $B_0$  is represented the applied magnetic field normal to the flow path. The main set of equations of nanofluids between two plates are given:

$$\frac{\partial u}{\partial x} + \frac{\partial v}{\partial y} + \frac{\partial w}{\partial z} = 0 \quad (1)$$

$$\rho_{\text{nf}} \left[ \frac{\partial u}{\partial t} + u \frac{\partial u}{\partial x} + v \frac{\partial u}{\partial y} + w \frac{\partial u}{\partial z} + \frac{2\Omega_0}{(1 - \alpha t)} w \right] = -\frac{\partial p}{\partial x} + \mu_{\text{nf}} \left( \frac{\partial^2 u}{\partial x^2} + \frac{\partial^2 u}{\partial y^2} + \frac{\partial^2 u}{\partial z^2} \right) - \frac{u}{(1 - \alpha t)} \left( \frac{\mu_{\text{nf}}}{k^\otimes} - \sigma_{\text{nf}} B_0^2 \right) + g(\rho\beta)_{\text{nf}} (T - T_0) \quad (2)$$

$$\rho_{\text{nf}} \left( \frac{\partial v}{\partial t} + u \frac{\partial v}{\partial x} + v \frac{\partial v}{\partial y} + w \frac{\partial v}{\partial z} \right) = -\frac{\partial p}{\partial y} + \mu_{\text{nf}} \left( \frac{\partial^2 v}{\partial x^2} + \frac{\partial^2 v}{\partial y^2} + \frac{\partial^2 v}{\partial z^2} \right) - \frac{\mu_{\text{nf}}}{k^\otimes} \frac{v}{(1 - \alpha t)} \quad (3)$$

$$\rho_{nf} \left[ \frac{\partial w}{\partial t} + u \frac{\partial w}{\partial x} + v \frac{\partial w}{\partial y} + w \frac{\partial w}{\partial z} - \frac{2\Omega_0}{(1-\alpha t)} w \right] = \mu_{nf} \left( \frac{\partial^2 w}{\partial x^2} + \frac{\partial^2 w}{\partial y^2} + \frac{\partial^2 w}{\partial z^2} \right) - \left( \frac{\mu_{nf}}{k^\otimes} + \sigma_{nf} B_0^2 \right) \frac{w}{(1-\alpha t)} \quad (4)$$

$$(\rho C_p)_{nf} \left[ \frac{\partial T}{\partial t} + u \frac{\partial T}{\partial x} + v \frac{\partial T}{\partial y} + w \frac{\partial T}{\partial z} \right] = k_{nf} \left( \frac{\partial^2 T}{\partial x^2} + \frac{\partial^2 T}{\partial y^2} + \frac{\partial^2 T}{\partial z^2} \right) \quad (5)$$

The velocity segments  $u$ ,  $v$ , and  $w$  are acting along the  $x$ -,  $y$ - and  $z$ -directions,  $T$  is the temperature, the acceleration due to gravity is represented by  $g$ ,  $\rho_{nf}$  – the density of the nanofluid,  $\mu_{nf}$  – the dynamic viscosity of the nanofluids,  $p$  – the show pressure,  $k^\otimes$  – the permeability,  $B_0$  – the represents the magnetic field,  $(\rho C_p)_{nf}$  – the heat capacitance of the nanofluid,  $k_{nf}$  – the thermal conductivity of the nanofluid. Where electrical conductivity of the nanofluid is represented by  $\sigma_{nf}$ .

The set of appropriate boundary conditions:

$$u = \frac{ax}{(1-\alpha t)} = U_w, \quad v = \frac{-V_0}{(1-\alpha t)}, \quad w = 0, \quad T = T_0 \quad \text{such that at } y = 0 \quad (6)$$

$$u = 0, \quad v = -\frac{\alpha}{2} \sqrt{\frac{\nu_f}{a(1-\alpha t)}}, \quad w = 0, \quad T = T_D \quad \text{such that at } y = D \quad (7)$$

The thermophysical constraints of the nanofluid [24]:

$$\begin{aligned} \rho_{nf} &= \rho_f (1-\phi) + \phi \rho_s, \quad \mu_{nf} = \frac{\mu_f}{(1-\phi)^{2.5}} \\ (\rho\beta)_{nf} &= (\rho\beta)_f (1-\phi) + \phi (\rho\beta)_s \\ (\rho C_p)_{nf} &= (\rho C_p)_f (1-\phi) + (\rho C_p)_s \\ \frac{k_{ns}}{k_f} &= \left( \frac{k_s + 2k_f - 2\phi(k_f - k_s)}{k_s + 2k_f + 2\phi(k_f - k_s)} \right) \end{aligned}$$

The subscripts (nf, f, s) represent the nanofluid, base fluid and solid particles, respectively.

The Von Karman [20] similarity transformation for the proposed problems have been used:

$$\begin{aligned} u &= \frac{ax}{(1-\alpha t)} f'(\eta), \quad w = \frac{axg}{(1-\alpha t)} h(\eta), \quad v = -\sqrt{\frac{a\nu_f}{(1-\alpha t)}} f(\eta) \\ D &= \sqrt{\frac{\nu_f(1-\alpha t)}{a}}, \quad \eta = \frac{y}{D}, \quad \Theta(\eta) = \frac{T - T_0}{(T_D - T_0)} \end{aligned} \quad (8)$$

Inserting eq. (8) into eqs. (2)-(5) the transform equations are obtained:

$$\begin{aligned} f^{iv} + (1-\phi)^{2.5} \left[ (1-\phi) + \phi \frac{\rho_s}{\rho_f} \right] \left[ f f''' - f' f'' - \frac{S}{2} (\eta f''' + 3f'') - 2\Omega h' \right] - \\ - M(1-\phi)^{2.5} f'' - Kr f'' + (1-\phi)^{2.5} \left[ (1-\phi) + \phi \frac{(\rho\beta)_s}{(\rho\beta)_f} \right] Gr \Theta' = 0 \end{aligned} \quad (9)$$

$$h'' + (1-\phi)^{2.5} \left\{ (1-\phi) + \phi \frac{\rho_s}{\rho_f} \right\} \left[ f h' - h f' - S \left( h + \frac{\eta}{2} h' \right) + 2\Omega f' \right] - Kr h - M(1-\phi)^{2.5} h = 0 \quad (10)$$

$$\frac{k_{nf}}{k_f} \Theta'' - \text{Pr} \left[ (1-\phi) + \phi \frac{(\rho C_p)_s}{(\rho C_p)_f} \right] \left[ S \left( \frac{\eta}{2} \Theta' \right) - f \Theta' \right] = 0 \quad (11)$$

where (') represent the differentiation. The non-dimensional parameters obtained as  $\delta = V_0/aD$ , unsteady parameter  $S = \alpha/a$ ,  $\text{Gr} = [g(\rho\beta)_{nf}(T_D - T_0(1 - at))]/\rho_f a U_w$  – the Grashoff number,  $\Omega = \Omega_0/a$  – the rotation parameter,  $M = \sigma_{nf} B_0^2/\rho_f a$  – the magnetic constraint,  $Kr = v_f/ak^\otimes$  – the porosity parameter, and the Prandtl number  $\text{Pr} = \mu_f(cp)_f/k_f$ , respectively. The simplified physical conditions:

$$\frac{df(0)}{d\eta} = 1, \quad f(0) = \delta, \quad h(0) = 0, \quad \Theta(0) = 1 \quad (12)$$

$$\frac{df(1)}{d\eta} = 0, \quad f(1) = \frac{S}{2}, \quad h(1) = 0, \quad \Theta(1) = 0 \quad (13)$$

The skin friction or the drag force

$$C_{fx} = \frac{-2\tau_w}{\rho_{nf} U_w^2}, \quad \tau_w = \mu_{nf} \left( \frac{\partial u}{\partial y} + \frac{\partial v}{\partial x} \right)_{y=0}$$

and the Nusselt number or heat transfer rate:

$$\text{Nu}_x = -\frac{xk_{nf}}{k_f (T_D - T_0)} \left( \frac{\partial T}{\partial y} \right)_{y=0}$$

are presented as [25], but there are the typo mistakes in the simplified form of the drag force and heat transfer rate. Therefore, the correct simplified form of the drag force and heat transfer rate:

$$C_{fx} (\text{Re}_x)^{1/2} = \frac{-2v_{nf}}{v_f} f''(0), \quad (\text{Re}_x)^{-1/2} \text{Nu}_x = -\frac{k_{nf}}{k_f} \Theta(0) \quad (14)$$

Here,  $\text{Re}_x = xU_w/v_f$  is the local Reynold number and  $v_{nf} = \mu_{nf}/\rho_{nf}$  – the kinematic viscosity of the nanofluid.

### Solution of the problem

To find an analytical solution we use OHAM procedure, eqs. (9)-(13) solved by a well-known and an efficient OHAM technique. The OHAM procedure gives a succession solution and in the first step the trial solution is selected which satisfies the physical conditions. The trial solution for the proposed problem is obtained:

$$f(\eta) = (2\delta - S + 1)\eta^3 + (3S - 6\delta - 4)\frac{\eta^2}{2} + \eta + \delta, \quad h(\eta) = 0, \quad \Theta(\eta) = 1 - \eta \quad (15)$$

The selected linear operators:

$$L_f = \frac{\partial^4 f}{\partial \eta^4}, \quad L_h = \frac{\partial^2 h}{\partial \eta^2}, \quad L_\Theta = \frac{\partial^2 \Theta}{\partial \eta^2} \quad (16)$$

The generalized linear operators:

$$L_f (c_1 + c_2\eta + c_3\eta^2 + c_4\eta^3) = 0, \quad L_h (c_5 + c_6\eta) = 0, \quad L_\Theta (c_7 + c_8\eta) = 0 \quad (17)$$

where  $c_1, c_2, \dots, c_8$  are arbitrary constant which is included in general solution. The  $k^{\text{th}}$  order approximation of average residual errors is introduced by Liao [25]:

$$\begin{aligned} \varepsilon_k^f(\tilde{h}_f) &= \frac{1}{N+1} \sum_{j=0}^N \left[ \sum_{i=0}^k (f_i)_{\eta=j\pi\eta} \right]^2 \\ \varepsilon_k^h(\tilde{h}_f, \tilde{h}_h) &= \frac{1}{N+1} \sum_{j=0}^N \left[ \sum_{i=0}^k (f_i)_{\xi=j\pi\eta}, \sum_{i=0}^k (h_i)_{\xi=j\pi\eta} \right]^2 \\ \varepsilon_k^\Theta(\tilde{h}_f, \tilde{h}_\Theta) &= \frac{1}{N+1} \sum_{j=0}^N \left[ \sum_{i=0}^k (f_i)_{\zeta=j\pi\eta}, \sum_{i=0}^k (\Theta_i)_{\zeta=j\pi\eta} \right]^2 \end{aligned} \quad (18)$$

According to Liao [25]  $\varepsilon^t = \varepsilon_k^f + \varepsilon_k^h + \varepsilon_k^\Theta$ . Here  $\varepsilon^t$  represents the total residual error. In the increasing order of approximation, the sum of the total square residual error has the tendency to rapidly converge the solution. The specified values of optimal control convergence parameters is  $\tilde{h}_f = -0.889633$ ,  $\tilde{h}_h = -0.924785$ ,  $\tilde{h}_\Theta = -0.623565$  in case of GO-EG, while  $\tilde{h}_f = -0.89084$ ,  $\tilde{h}_h = -0.92862$ ,  $\tilde{h}_\Theta = -0.597822$  in case of GO-W.

**Result and discussion**

The two sorts of (GO-W and GO-EG) nanofluids flow amongst the two uprights and parallel plates for the heat transfer enhancement applications is analyzed in this research. The geometry of the problem is displayed in fig. 1. The solution of the problem has been obtained through OHAM technique using the BVP 2.0 package up to the 20<sup>th</sup> order approximation.

*Velocity profiles:* The impact of the embedded parameters over the radial and azimuthal velocity profiles for the GO-W/GO-EG nanofluids were examined physically in figs. 2-9. Figures 2 and 3 demonstrate the influence of magnetic parameter,  $M$ , vs. velocity pitch  $f'(\eta)$  for the GO-W/GO-EG nanofluids. The greater amount of the volume fraction,  $\phi$ , increases the thermal properties of the nanofluid and the viscous forces become feeble to stop the fluid-flow, also the kinetic energy of the molecules increases. Therefore, the larger values of the nanoparticle,  $\phi$ , rise the radial and azimuthal velocities as shown in figs. 4 and 5. Figures 6 and 7 demonstrate the impact of the porosity constraint,  $Kr$ , on the velocity outlines,  $f'(\eta)$  and  $h(\eta)$ , comprising GO-W/GO-EG nanofluids. The effect of the unsteadiness parameter,  $S$ , vs. velocity fields,  $f'(\eta)$

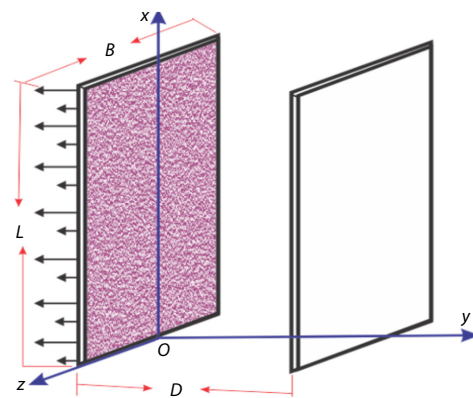


Figure 1. Physical sketch of the problem for the nanofluid flow

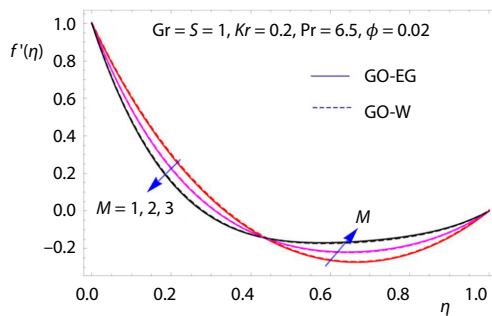


Figure 2. Magnetic parameter vs.  $f'(\eta)$

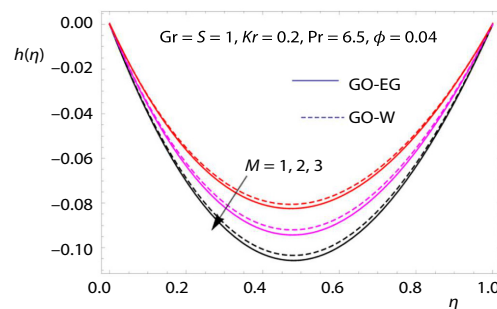


Figure 3. Magnet parameter vs.  $h(\eta)$

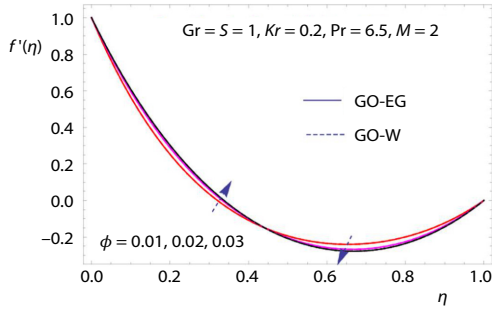


Figure 4. Nanoparticle volume fraction  $\phi$  vs.  $f'(\eta)$

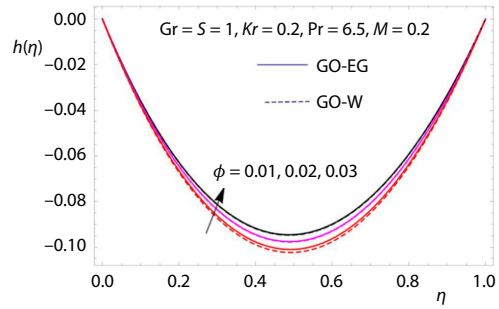


Figure 5. Nanoparticle volume fraction  $\phi$  vs.  $h(\eta)$

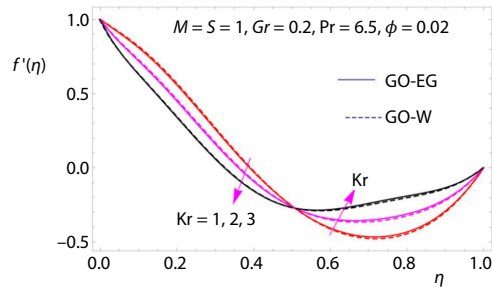


Figure 6. Porosity Parameter  $Kr$  vs.  $f'(\eta)$

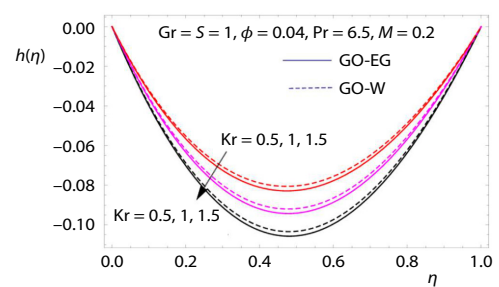


Figure 7. Porosity parameter  $Kr$  vs.  $h(\eta)$

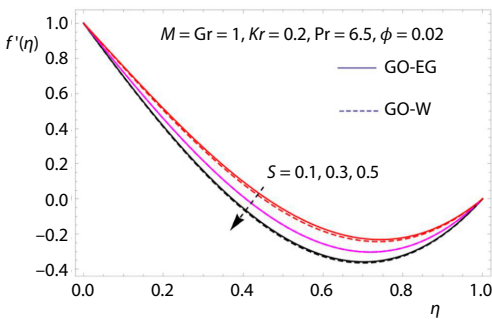


Figure 8. Unsteady parameter  $S$  vs.  $f'(\eta)$

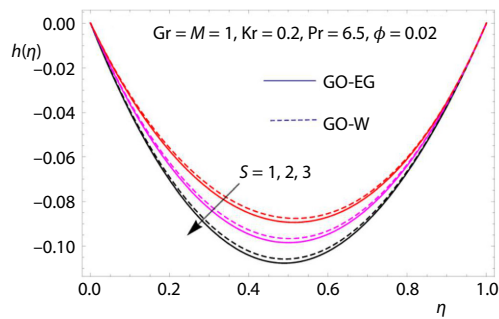


Figure 9. Unsteady parameter  $S$  vs.  $h(\eta)$

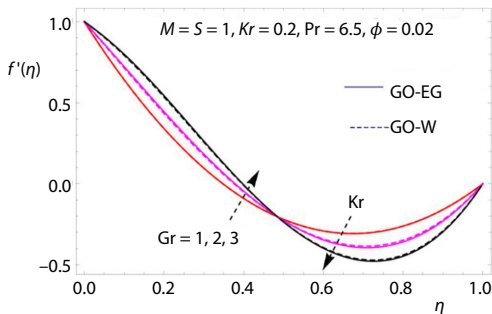


Figure 10. Grashop number vs.  $f'(\eta)$

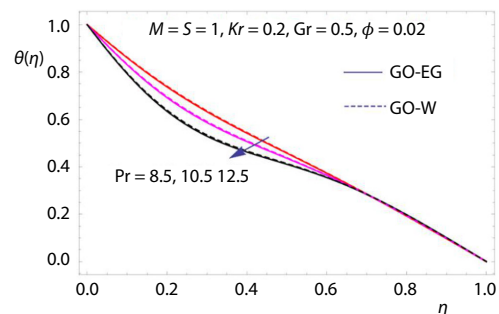


Figure 11. Prandtl number vs.  $\Theta(\eta)$

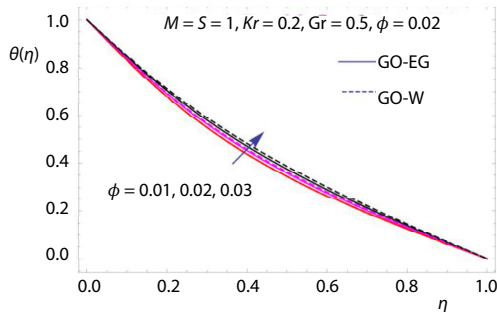


Figure 12. Nanoparticle volume fraction  $\phi$  vs.  $\Theta(\eta)$

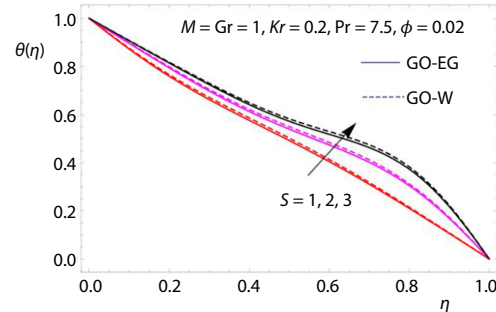


Figure 13. Unsteady parameter  $S$  vs.  $\Theta(\eta)$

and  $h(\eta)$ , for both sorts of nanofluids GO-W/GO-EG has been displayed in figs. 8 and 9. The influence of the Grashof number vs. the radial velocity has been depicted in fig. 10.

**Temperature profile:** The changes in temperature field with different embedded parameters of GO-W/GO-EG nanofluids have been depicted in figs. 11-13. Figure 11 depicts the temperature field for varying values of Prandtl number in the existence of GO-W/GO-EG nanofluids. It is obvious that Prandtl number enhances due to decelerating the thermal boundary-layer. The decline effect is relatively strong in GO-EG nanofluid as compared to GO-W nanofluid. Figure 12 shows the variation in the temperature field with the fluctuation in the volume fraction,  $\phi$ . Temperature field increases due to the rising value of  $\phi$  for both sorts of GO-W/GO-EG nanofluids. Figure 13 witnesses the influence of unsteadiness parameter in the temperature profile.

Table 1. The experimental value of the base solvents and material existing in literature

Model	$\rho$ [ $\text{kgm}^{-3}$ ]	$C_p$ [ $\text{Jkg}^{-1}\text{K}^{-1}$ ]	$K$ [ $\text{Wm}^{-1}\text{k}^{-1}$ ]
Water	997.1	4179	0.613
Graphene oxide	1800	717	5000
Ethylene glycol	1.115	0.58	0.1490

Table 2. The sum of the total squared residual errors for GO-W when  $\text{Pr} = 6.7$ ,  $Kr = M = S = \text{Gr} = 0.1$ ,  $\phi = 0.03$

$m$	$\epsilon_m^f \text{GO-W}$	$\epsilon_m^h \text{GO-W}$	$\epsilon_m^\theta \text{GO-W}$
6	$1.54192 \cdot 10^{-6}$	$7.97335 \cdot 10^{-9}$	$2.9728 \cdot 10^{-3}$
12	$2.66015 \cdot 10^{-13}$	$6.33566 \cdot 10^{-16}$	$3.21951 \cdot 10^{-7}$
18	$7.34959 \cdot 10^{-20}$	$1.30031 \cdot 10^{-22}$	$8.73192 \cdot 10^{-11}$
24	$2.71757 \cdot 10^{-26}$	$3.93722 \cdot 10^{-29}$	$4.52021 \cdot 10^{-15}$
30	$1.42407 \cdot 10^{-29}$	$1.11747 \cdot 10^{-33}$	$1.90803 \cdot 10^{-20}$

is relatively fast in the GO-EG nanofluid. In tab. 4 the declining values of the unsteady parameter,  $S$ , reduce the skin friction,  $f''(0)$ . The larger values of  $Kr$  decline the skin frictions,  $f''(0)$ , as shown in tab. 4 for both types of nanofluids GO-W/GO-EG nanofluids, respectively. Table 5 represents heat transfer rate. Physically the larger amount of nanoparticle volume fraction utilized for the heat transfer enhancement. Therefore, the rising values of  $\phi$  decline the cooling effect. Similarly, the increasing values of the unsteady parameter  $S$  increasing the temperature field while its decreasing values enhancing the heat transfer rate as shown in tab. 5. The temperature field decreases with larger amount of Prandtl value and cooling effect improves as depicted in tab. 5.

**Numerical results:** The experimental values of the base solvents and materials revealed in tab. 1. Tables 2 and 3 represent the individual's average square residual error of ethylene GO-EG and GO-W executed in a different order of approximation. We also noticed that average square residual error value can be reduced by increasing the order of approximation. In tab. 4 the impact of the various physical parameters vs. skin fractions,  $f''(0)$ , have been examined. The larger value of the local Reynolds number improving the inertial effect and as a result the  $f''(0)$  increases. Further, this effect

**Table 3. The sum of the total squared residual errors for GO-EG when  $Pr = 6.7, Kr = M = S = Gr = 0.1, \phi = 0.03$** 

$m$	$\varepsilon_m^f$ GO-W	$\varepsilon_m^h$ GO-W	$\varepsilon_m^p$ GO-W	$\varepsilon_m^\theta$ GO-W
6	$1.60937 \cdot 10^{-6}$	$8.8119 \cdot 10^{-9}$	$3.06286 \cdot 10^{-6}$	$3.66276 \cdot 10^{-3}$
12	$2.90818 \cdot 10^{-13}$	$7.32854 \cdot 10^{-16}$	$2.47455 \cdot 10^{-6}$	$5.04955 \cdot 10^{-7}$
18	$8.37103 \cdot 10^{-20}$	$1.55859 \cdot 10^{-22}$	$2.47458 \cdot 10^{-6}$	$1.7076 \cdot 10^{-11}$
24	$3.07644 \cdot 10^{-26}$	$5.03387 \cdot 10^{-29}$	$2.47458 \cdot 10^{-6}$	$1.17028 \cdot 10^{-15}$
30	$2.26584 \cdot 10^{-32}$	$5.43794 \cdot 10^{-33}$	$2.47458 \cdot 10^{-6}$	$6.08747 \cdot 10^{-20}$

**Table 4. Impact of the physical parameters vs.  $-f''(0)$** 

$Re_x$	$S$	$Kr$	$f''(0)$ GO-W	$f''(0)$ GO-EG
0.1	0.9	0.8	6.22547	6.46264
0.2			6.81442	7.55048
	0.8		6.19352	6.41735
	0.7		6.16159	6.3721
		0.9	6.20244	6.42399
		1.0	6.17947	6.3855

**Table 5. Impact of the physical parameters vs. heat transfer rate  $\theta'(0)$** 

$S$	$Pr$	$\phi$	$\theta'(0)$ GO-W	$\theta'(0)$ GO-EG
0.9	0.7	0.01	1.84951	1.84066
0.8			1.85055	1.84169
0.7			1.85159	1.84271
	0.8		1.84967	1.84085
	0.9		1.84983	1.84104
		0.02	1.86498	1.84688
		0.03	1.85387	1.83477

## Conclusion

In current article we examine, unsteady incompressible MHD 3-D GO-W and GO-EG nanofluid-flow passed through a permeable medium limited by two vertical plates. The two types of nanofluids, GO-W and GO-EG, have been used in the mathematical model for the heat transfer enhancement applications. The proposed problem is solved by the well-known OHAM method for the velocity profiles and temperature field. Radial and azimuthal velocity profiles depreciated with the larger values of the magnetic field, porosity parameter, unsteady parameter, Reynolds number. The radial and azimuthal velocity pitches are increasing with the rising value of the volume fraction. Temperature distribution running down to Prandtl number and running up for volume fraction. The numerical outputs show that at the 30<sup>th</sup> order approximation the obtained residual error tends to  $6.08747 \cdot 10^{-20}$  which show the strong convergence of the non-linear problem.

## Acknowledgment

This project was funded by the Deanship of Scientific Research (DSR), King Abdulaziz University, Jeddah, SA under grant no. (KEP-18-130-19). The authors, therefore, acknowledge with thanks DSR technical and financial support.

## References

- [1] Choi, S. U. S., et al., Developments and Applications of Non-Newtonian Flows, *ASME FED*, 66 (1995), Nov., pp. 99-105
- [2] Choi, S. U. S., et al., Anomalous Thermal Conductivity Enhancement in Nanotube Suspensions, *Applied Physics Letters*, 79 (2001), Sept., pp. 2252-2254
- [3] Buongiorno, J., Convective Transport in Nanofluids, *Journal of heat transfer*, 128 (2006), Aug., pp. 240-250
- [4] Timofeeva, E. V., et al., Particle Shape Effects on Thermophysical Properties of Alumina Nanofluids, *Journal of Applied Physics*, 106 (2009), July, 014304
- [5] Maxwell, J. C., A Treatise on Electricity and Magnetism, *Clarendon Press*, 1 (1881)
- [6] Jeffrey, D. J., Conduction through a Random Suspension of Spheres, *Proceedings of the Royal Society of London, Series A, Mathematical and Physical Sciences*, (1973), pp. 355-367
- [7] Davis, R. H., The Effective Thermal Conductivity of a Composite Material with Spherical Inclusions, *Int. J. of Thermophysics*, 7 (1986), 3, pp. 609-620
- [8] Lu, S. Y., Lin, H. C., Effective Conductivity of Composites Containing Aligned Spheroidal Inclusions of Finite Conductivity, *Journal of Applied Physics*, 79 (1996), 9, pp. 6761-6769
- [9] Hamilton, R. L., Crosser, O. K., Thermal Conductivity of Heterogeneous Two-Component Systems, *Industrial and Engineering Chemistry Fundamentals*, 1 (1962), 3, pp. 187-191
- [10] Sheikholeslami, M., Ganji, D. D., Nanofluid-Flow and Heat Transfer between Parallel Plates Considering Brownian Motion Using DTM, *Computer Methods in Applied Mechanics and Engineering*, 283 (2015), Jan., pp. 651-663
- [11] Sheikholeslami, M., Ganji, D. D., Heat Transfer of Cu-water Nanofluid-Flow between Parallel Plates, *Powder Technology*, 235 (2013), Feb., pp. 873-879
- [12] Sheikholeslami, M., Ganji, D. D., Entropy Generation of Nanofluid in Presence of Magnetic Field Using Lattice Boltzmann Method, *Physica A: Stat. and Its Application*, 417 (2015), Jan., pp. 273-286
- [13] Sheikholeslami, M., et al., Nanofluid-Flow and Heat Transfer in a Rotating System in the Presence of a Magnetic Field, *Journal of Molecular Liquids*, 190 (2014), Feb., pp. 112-120
- [14] Mahmoodi, M., Kandelousi, S., Analysis of the Hydrothermal Behavior and Entropy Generation in a Regenerative Cooling Channel Considering Thermal Radiation, *Nuclear Engineering and Design*, 291 (2015), Sept., pp. 277-286
- [15] Ellahi, R., et al., Shape Effects of Nanosize Particles in Cu-H<sub>2</sub>O Nanofluid on Entropy Generation, *Int. J. of Heat and Mass Transfer*, 81 (2015), Feb., pp. 449-456
- [16] Akbar, N. S., Butt, A. W., Ferromagnetic Effects for Peristaltic Flow of Cu-water Nanofluid for Different Shapes of Nanosize Particles, *Applied Nanoscience*, 6 (2016), Mar., pp. 379-385
- [17] Ellahi, R., et al., The Shape Effects of Nanoparticles Suspended in HFE-7100 over Wedge with Entropy Generation and Mixed Convection, *Applied Nanoscience*, 6 (2016), May, pp. 641-651
- [18] Sheikholeslami, M., et al., Steady Nanofluid-Flow between Parallel Plates Considering Thermophoresis and Brownian Effects, *Journal of King Saud University-Science*, 28 (2016), Oct., pp. 380-389
- [19] Mahmoodi, M., Kandelousi, S., Application of DTM for Kerosene-Alumina Nanofluid-Flow and Heat Transfer between Two Rotating Plates, *The Eur. Phys. J. Plus*, 130 (2015), July, p. 142
- [20] Karman, T. V., Uber Laminare und Turbulente Reibung, *ZAMM Journal of Applied Mathematics and Mechanics/Zeitschrift für Angewandte Mathematik und Mechanik*, 1 (1921), 4, pp. 233-252
- [21] Sheikholeslami, M., Ganji, D. D., The 3-D Heat and Mass Transfer in a Rotating System Using Nanofluid, *Powder Technology*, 253 (2014), Feb., pp. 789-796
- [22] Rashidi, M. M., et al., Influences of an Effective Prandtl Number Model on Nanoboundary-Layer Flow of  $\gamma\text{Al}_2\text{O}_3\text{-H}_2\text{O}$  and  $\gamma\text{Al}_2\text{O}_3\text{-C}_2\text{H}_6\text{O}_2$  over a Vertical Stretching Sheet, *Int. Journal of Heat and Mass Transfer*, 98 (2016), July, pp. 616-623
- [23] Ahmed, N., et al., Influence of an Effective Prandtl Number Model on Squeezed Flow of  $\gamma\text{Al}_2\text{O}_3\text{-H}_2\text{O}$  and  $\gamma\text{Al}_2\text{O}_3\text{-C}_2\text{H}_6\text{O}_2$  Nanofluids, *Journal of Molec. Liq.*, 238 (2017), July, pp. 447-454
- [24] Azimi, M., et al., Investigation of the Unsteady Graphene Oxide Nanofluid-Flow between Two Moving Plates, *Journal of Computational and Theoretical Nanoscience*, 11 (2014), Oct., pp. 2104-2108
- [25] Liao, S., An Optimal Homotopy-Analysis Approach for Strongly Non-Linear Differential Equations, *Commun. in Non. Sc. and Num. Simuln*, 15 (2010), Aug., pp. 2003-2016